Open Access Journal
Journal of Power Technologies 94 (Nuclear Issue) (2014) 1–7
journal homepage:papers.itc.pw.edu.pl

Wall temperature prediction in annular geometry during post-dryout heat transfer

Ionut G. Anghel*, Henryk Anglart

Royal Institute of Technology (KTH)
Roslagstullsbacken 21, 106 91 Stockholm, Sweden

Abstract

In this paper a new approach to predict wall temperature during post-dryout heat transfer in annuli with flow obstacles is presented. The proposed approach takes into account the obstacle specifics and location in the channel to determine the onset of post-dryout patch. The wall temperature in the dry patch area is predicted from a correlation that takes into account the developing post-dryout heat transfer regime. The method is applied to post-dryout conditions in an annulus with pin spacers and achieves a significant improvement in prediction accuracy compared to other reference methods.

Keywords: Post-dryout, Obstacle effect, Annular geometry, Heat transfer

1. Introduction

The post-dryout heat transfer regime may occur in fuel rod bundles of Boiling Water Reactors (BWR) when the local power level becomes critical. This type of violation of safety limit conditions practically never occurs under stationary reactor operation conditions, since adequate thermal margins are applied. Under certain transient conditions the occurrence of post-dryout is more probable and thus adequate safety margins are required to avoid this type heat transfer anomaly. The post-dryout exclusion approach is adopted in most licensing procedures to avoid reactor shutdown for the purpose of inspecting fuel for possible clad damage. This requirement is motivated by the fact that clad temperature prediction is very uncertain under post-dryout conditions and that temperature levels are believed to rapidly exceed the clad damage limit.

Post-dryout heat transfer has been intensively investigated in electrically-heated test sections in the past. Both obstacle-free and channels with flow obstacles have been employed. Becker et al. [1] performed wall temperature measurements in a vertical, obstacle-free pipe with inner diameter 15 mm and length 7 m. Their measurements covered a wide range of operating pressures (3 to 20 MPa) and mass fluxes (500 to 3000 kg/m^{2}s). Anghel and Anglart [2] measured wall temperature in a vertical annulus with pin spacers and with inner/outer diameters 12.7/24.3 mm and with length 3.65 m. They investigated post-dryout heat transfer for pressures from 5 to 9 MPa and mass fluxes from 500 to 1750 kg/m^{2}s.

Experimental results obtained in obstacle-free pipes are very valuable due to the simplicity of the geometry, which allows for a thorough study of the governing phenomena. However, conditions ob-

*Corresponding author
Email addresses: iganghel@kth.se (Ionut G. Anghel*), henryk@kth.se (Henryk Anglart)

tained in heated pipes do not correspond to the conditions that can be expected in fuel assemblies of nuclear reactors. In particular, the critical quality for heated tubes is significantly higher than the critical quality for heated rods. Accordingly, correlations developed with data obtained from tubes are in general not applicable to channels containing heated rods, such as nuclear fuel assemblies. In addition, fuel assemblies always have flow obstacles, such as grid spacers, which significantly modify the phase distribution in the flow cross-section.

This paper is concerned with prediction of wall temperature during post-dryout heat transfer in channels with flow obstacles, such as BWR fuel assemblies. Major experimental findings are summarized in Section 2. Section 3 contains comparisons of measured [1, 2] and calculated [3, 4] wall temperatures during post-dryout heat transfer in pipes and annuli. The effect of flow obstacles on post-dryout heat transfer is discussed in Section 4.

2. Measured wall temperature

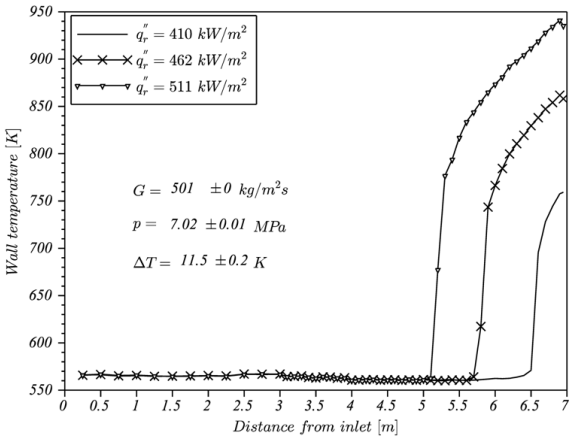

Figure 1: Measured [1] wall temperature versus axial distance in a 15 mm ID uniformly heated pipe at low mass flux conditions

Figures 1 through 4 show the measured wall temperature in a pipe and in an annulus with pin spacers. Fig. 1 shows the pipe wall temperature distributions at three heat flux levels, keeping all other parameters constant. In all three cases the wall temperature monotonically increases with distance in the

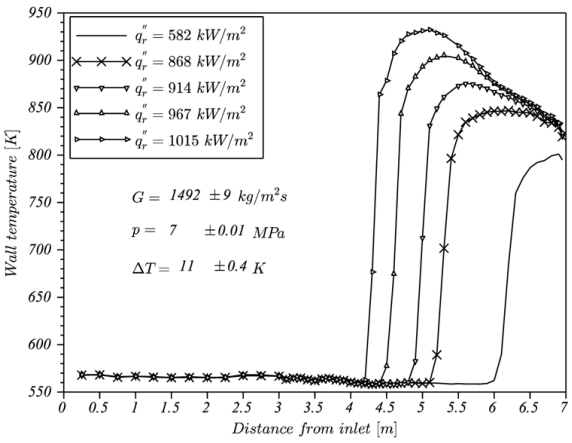

Figure 2: Measured [2] wall temperature versus axial distance in a 15 mm ID uniformly heated pipe at high mass flux conditions

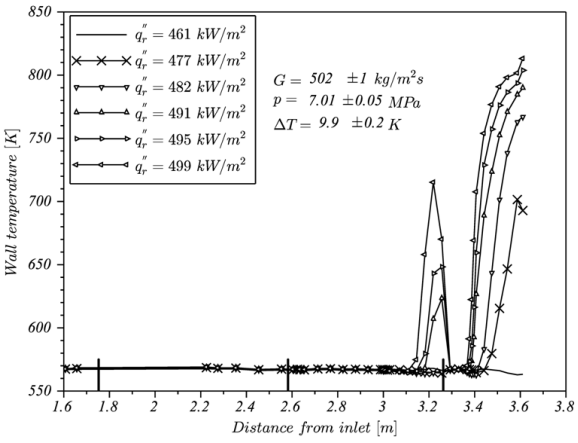

Figure 3: Measured [2] rod wall temperature versus axial distance in a 12.7/24.3 mm ID/OD uniformly heated annulus with pin spacers at low mass flux conditions

post-dryout region. The rapid wall temperature increase just downstream of the dryout point is due to a transition from the convective boiling heat transfer to the post-dryout heat transfer regime. Further downstream, close to the exit from the test section, the almost linear increase in wall temperature corresponds to a single-phase convection heat transfer to superheated vapor.

For high mass fluxes the wall temperature pattern in the post-dryout region changes significantly, as can be observed in Fig. 2. As with low mass fluxes, the wall temperature rapidly increases just down-

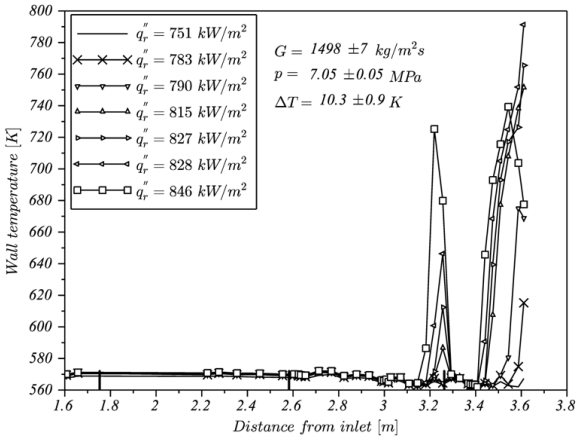

Figure 4: Measured [2] rod wall temperature versus axial distance in a 12.7/24.3 mm ID/OD uniformly heated annulus with pin spacers at high mass flux conditions

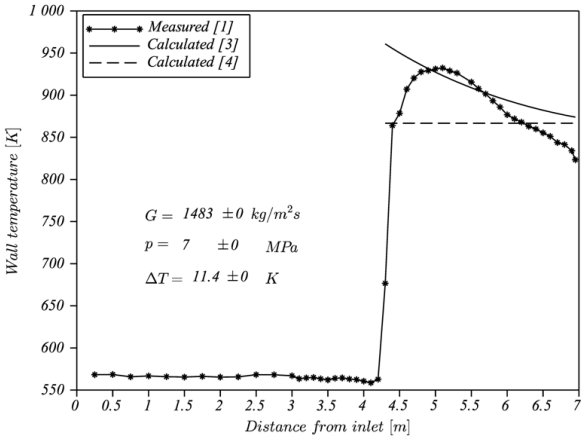

Figure 5: Calculated and measured wall temperature in a pipe with an inner diameter of 15 mm

stream of the onset of the dryout point. However, in the exit region of the test section (between 6 and 7 m from the inlet), the wall temperature decreases almost linearly with the axial distance. This behavior is caused by improved heat transfer conditions due to increasing average flow velocity of the mixture. The latter is caused by expansion of the mixture due to an intensive volumetric evaporation of droplets in the superheated steam.

The wall temperature distributions in the annular test section for low and high mass fluxes are shown in Fig. 3 and 4, respectively. The last pin spacer located at the distance of 3.26 m from the inlet causes a complete rewetting of the dry patch created upstream of its location. This effect persists for both low and high mass flux conditions and effectively prevents such wall temperature development as observed in Fig. 1 and 2.

The temperature patterns shown in Fig. 3 and 4 clearly indicate that several dry patches in channels with flow obstacles can be created. This behavior suggests that the onset of each dry patch should be governed by upstream conditions, such as distance to the flow obstacle, equilibrium quality at the obstacle location and local heat flux.

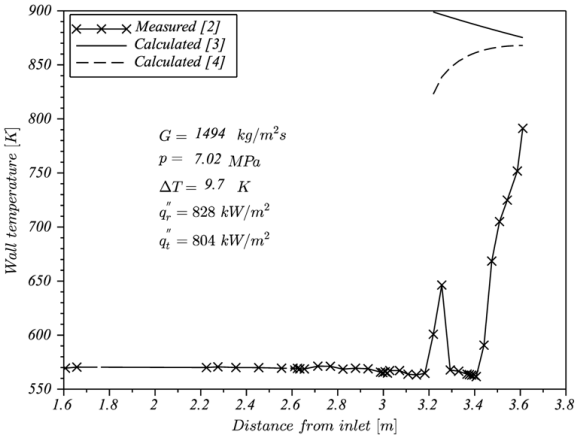

Figure 6: Calculated and measured inner wall temperature in an annulus with an inner/outer diameter of 12.7/24.3 mm

3. Calculated wall temperature

Various methods to calculate a wall temperature at post-dryout heat transfer conditions have been developed in the past. A short summary and description of such methods was given recently by Anghel and Anglart [2]. Two computational methods are employed in the present paper: the Groeneveld correlation [3] and the Saha model [4]. Both approaches are compared to the measured data in a pipe and in an annulus, as shown in Fig. 5 through 10. The wall temperature calculations are performed only in the post-dryout region, starting from the first appearance of a dry patch. As shown in Fig. 5, reasonable agree-

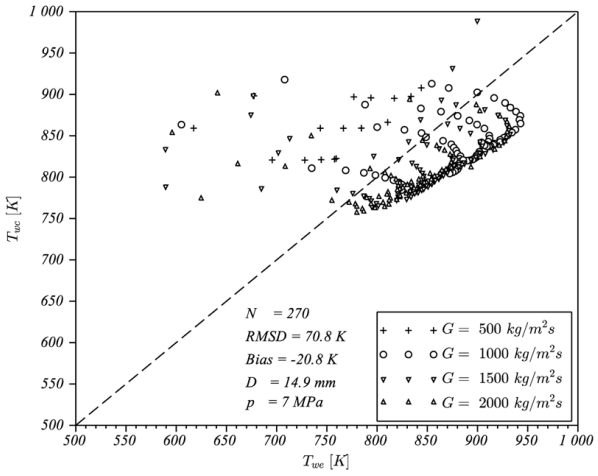

Figure 7: Comparison of measured [1] and calculated [3] wall temperature in a pipe with a diameter of 14.9 mm at pressure 7 MPa

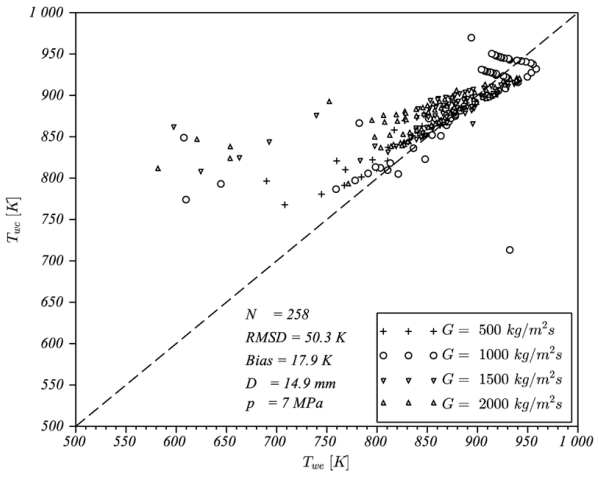

Figure 8: Comparison of measured [1] and calculated [4] wall temperature in a pipe with a diameter of 14.9 mm at pressure 7 MPa

ment between the measured and the calculated temperature is obtained for both methods, even though the axial shape of the wall temperature is not captured. However, a significant over-prediction of the wall temperature can be seen in Fig. 6. This should not be surprising, since no spacer effect is included in the calculations. Fig. 6 merely indicates that this effect must be taken into account in calculations in order to obtain reasonable agreement between exper-

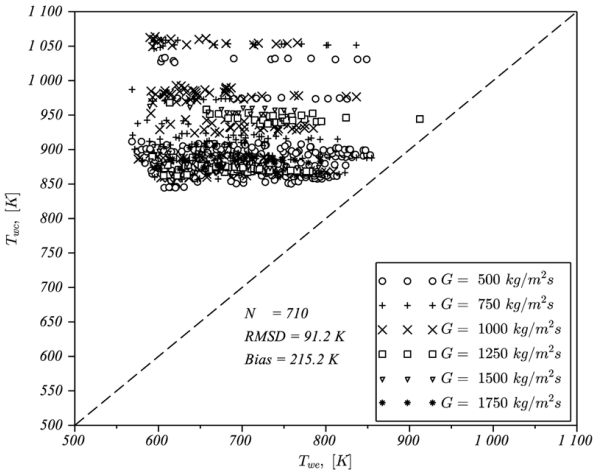

Figure 9: Comparison of measured [2] and calculated [3] wall temperature in an annulus with pin spacers

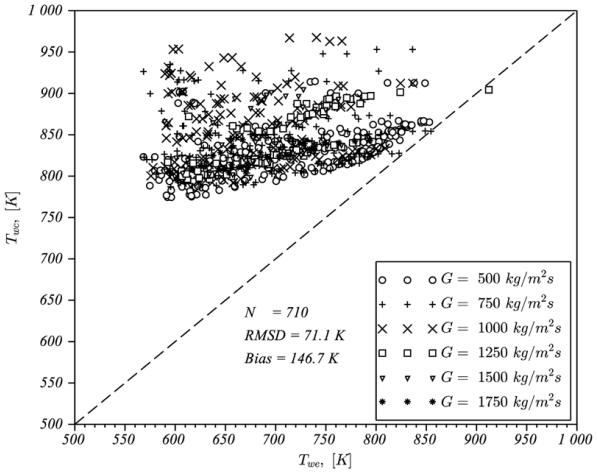

Figure 10: Comparison of measured[2] and calculated [4] wall temperature in an annulus with pin spacers

imental data and predictions.

Figures 7 and 8 show a comparison of the measured wall temperature in a pipe [1] with the calculated wall temperature using the Groeneveld correlation [3] and the Saha model [4], respectively. The reported unbiased root mean square deviation (RMSD) is defined as,

$$\Delta T_{wRMS} = \left[\frac{1}{N-1} \sum_{1}^{N} (T_{wc} - T_{we} - \Delta T_{wm}) \right]^{\frac{1}{2}} \quad (1)$$

where T_{we} and T_{wc} are the measured and the calculated wall temperature, respectively, N is the number of experimental data points and ΔT_{wm} is the mean deviation (bias) calculated as,

$$\Delta T_{wm} = \frac{1}{N} \sum_{1}^{N} (T_{wc} - T_{we}) \tag{2}$$

Figure 7 indicates that the calculated wall temperature is on average slightly lower than the measured temperature (negative bias). Figure 5 suggests that this is due mainly to under-prediction of the peak wall temperature in the post-dryout region. A relatively high RMSD (70.8 K) results from a significant over-prediction of the wall temperature in the region just downstream of the dry patch onset point.
As can be seen in Fig. 8 RMSD is slightly reduced (50.3 K) when the Saha model is used. This is mainly due to more accurate prediction of the wall temperature in the developing region of the post-dryout heat transfer regime.

Figures 9 and 10 show a comparison of calculated and measured wall temperature in an annulus with pin spacers for a sample of $N = 710$ experimental points in the following parameter range: mass flux from 500 to 1750 kg/m^{2}s, pressure from 5 to 7 MPa and inlet subcooling from 8 to 40 K. It is evident that both prediction methods significantly over-estimate the wall temperature, with a bias as high as 215.2 K in the case of the Groeneveld correlation. A slightly lower bias (146.7 K) was obtained when using the Saha model. The discrepancy between predictions and measurements stems mainly from the failure of both approaches to capture the wall temperature in the transition region from the onset of dryout point to the maximum wall temperature point.
Figures 9 and 10 indicate that to improve the overall accuracy of prediction of post-dryout heat transfer in channels with flow obstacles it is necessary to better capture the wall temperature development in the region just after the point of the onset of a dry patch. Anghel and Anglart [2] proposed the following correlation to calculate the local Nusselt number in that region:

$$Nu = Nu_o \left(1 + ae^{-b(x-x_{cr})}\right) \tag{3}$$

where Nu_o is obtained from the Saha model [4], x is the local equilibrium quality and x_{cr} is the closest upstream critical quality. Applying Eq. (3) to the data shown in Fig. 10, and using $a = 5.87$ and $b = 79.81$ (valid for the annular test section with pin spacers [5]) a significantly reduced bias is obtained, as shown in Fig. 11.

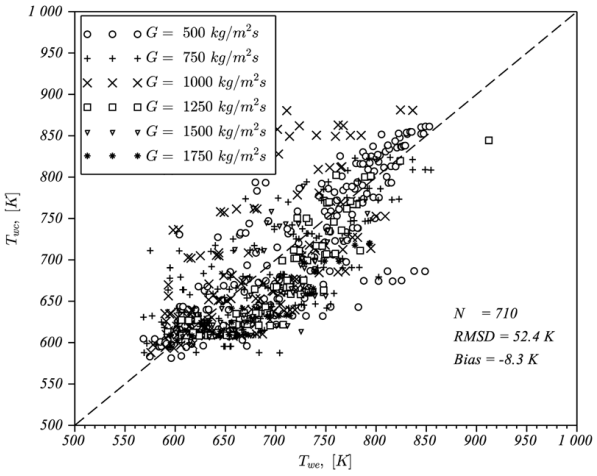

Figure 11: Comparison of measured [2] and calculated (Eq. 3) wall temperature in an annulus with pin spacers

The Saha model and Eq. (3) require the value of the critical quality in order to calculate the local wall temperature in the post-dryout region. The measured critical quality was used in the results shown in Fig. 10 and 11. In general, however, an additional correlation is needed to find this quality. Usually such correlations are derived from dryout experimental data obtained in the same geometry, assuring that the influence of possible flow obstacles is taken into account.

4. Effect of flow obstacles

Flow obstacles have a significant impact on post-dryout heat transfer due to several effects. The first important one is the translation and/or rewetting of a drypatch. This effect is clearly visible in Fig. 3 and 4, where dry patches developed upstream of the last pin spacer are rewetted directly downstream of its location. The rewetting phenomenon has a significant impact on the local wall temperature, since pre-dryout convective boiling heat transfer is re-established and the local wall temperature

is brought back to values close to the saturation liquid temperature. Figure 6 suggests that the wall temperature can be reduced as much as 200 K due to rewetting. The second effect of flow obstacles is to intensify heat transfer without rewetting, due to increased turbulence downstream of their locations. In such cases the reduction in wall temperature is not as high as with rewetting, but it is still quite significant.

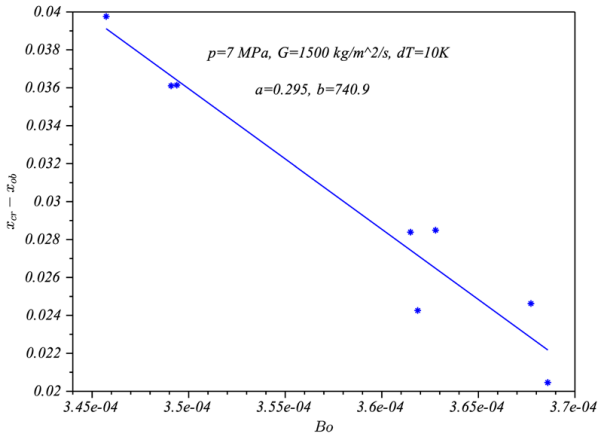

Figure 12: Critical quality relationship for the last pin spacer in the annular test section

The rewetting phenomenon can be investigated for each obstacle separately. In particular, one can develop a separate critical quality correlation, which will be used to predict the onset and location of the dry patch downstream of each obstacle. The critical quality can be expressed in terms of the boiling number Bo as follows,

$$x_{cr} = x_{ob} + A - B \cdot Bo, \quad Bo = \frac{q''}{\left(G \cdot i_{fg}\right)} \tag{4}$$

where x_{ob} is the equilibrium quality at the obstacle location, q'' is the wall heat flux, G is the mass flux and i_{fg} is the latent heat. Non-dimensional parameters A and B are in general functions of the mass flux, the pressure and the inlet subcooling that can be determined from experimental data. Fig. 12 shows the relationship (4) obtained for the last pin spacer in the annular test section and for selected operational conditions, p = 7 MPa, G = 1500 kg/m^{2}s and ΔT = 10 K. Thus, the following expression is obtained,

$$x_{cr} = x_{ob} + 0.295 - 740.9 \cdot Bo \tag{5}$$

A similar analysis performed for the same operational conditions gives the following expression for the penultimate pin spacer,

$$x_{cr} = x_{ob} + 0.095 - 40.9 \cdot Bo \tag{6}$$

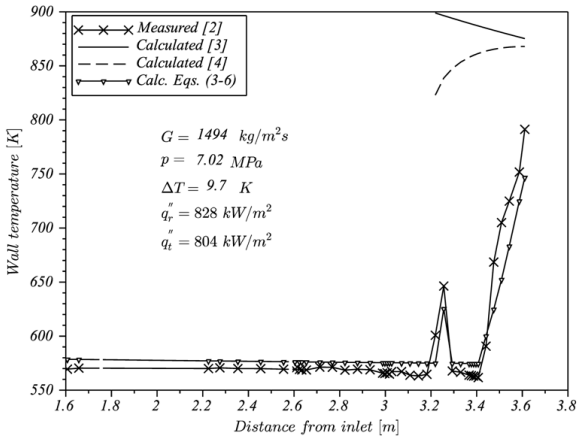

Figure 13: Calculated and measured inner wall temperature in an annulus with an inner/outer diameter of 12.7/24.3 mm

Equations (3) through (6) were used to predict the wall temperature in an annulus with pin spacers. A comparison of predicted and measured wall temperature is shown in Fig. 13. The Chen correlation was used to calculate the wall temperature in non-dryout regions. As can be seen, the accuracy of the new method is very good and the calculated wall temperature follows the same pattern as the measured temperature.

5. Conclusions

A new method to predict post-dryout heat transfer has been developed and demonstrated using experimental data obtained by Anghel and Anglart in an annular test section with pin spacers. The method employs a separate critical quality correlation for each flow obstacle, which is used to predict the onset and location of the dry patches. The critical quality correlations are geometry-specific and have to be obtained for each geometry from experimental data. The wall temperature evolution downstream of the onset of

dryout point can be calculated from the generic expression given by Eq. 3. The new methods make it possible to capture significantly more accurately the wall temperature during post-dryout heat transfer in channels with flow obstacles.

Acknowledgments

The publication was created within the framework of a strategic project of the Polish National Center for Research and Development (NCBR): "Technologies for the development of safe nuclear energy", Research Task No. 9 titled "Development and implementation of safety analysis methods in nuclear reactors during disturbances in heat removal and severe accident conditions".

References

[1] K. M. Becker, C. H. Ling, S. Hedberg, G. Strand, An experimental investigation of post dryout heat transfer, KTH-NEL-33 (1983).

[2] I. G. Anghel, H. Anglart, Post-dryout heat transfer to high-pressure water flowing upward in vertical channels with various flow obstacles, Int. J. Heat Mass Transfer 55 (2012) 8020–8031.

[3] D. C. Groeneveld, Post-dryout heat transfer at reactor operating conditions, AECL-4513 (1973).

[4] P. Saha, A nonequilibrium heat transfer model for dispersed droplet post-dryout regime, Int. J. Heat Mass Transfer 23 (1980) 438–492.

[5] I. G. Anghel, H. Anglart, On post-dryout heat transfer in channels with flow obstacles, Nuclear Engineering and Design 270 (2014) 351–358.

[6] J. C. Cohen, Correlation for boiling heat transfer to saturated fluids in convective flows, Eng. Chem. Des. Dev. 5 (3) (1966) 322–339.